IEEE Access
Multidisciplinary ⋮ Rapid Review ⋮ Open Access Journal

Received 3 November 2023, accepted 3 December 2023, date of publication 18 December 2023,
date of current version 28 December 2023.

Digital Object Identifier 10.1109/ACCESS.2023.3343842

RESEARCH ARTICLE

Pseudo-Random Signal Injection for Position Sensorless Control of Five-Phase IPMSM Based on Third Harmonic Space

YUHAO ZHANG[1], CHEN CHEN[2], ZHENGMENG LIU[1], (Member, IEEE), QIAN CHEN[1], (Senior Member, IEEE), JIAHAO ZHANG[1], AND GUOHAI LIU[1], (Senior Member, IEEE)

[1]School of Electrical and Information Engineering, Jiangsu University, Zhenjiang 212013, China
[2]China Nuclear Power Engineering Company Ltd., Beijing 100840, China

Corresponding author: Zhengmeng Liu (lzm@ujs.edu.cn)

This work was supported in part by the National Natural Science Foundation of China under Grant 52377054, Grant 51877098, and Grant 52077097; in part by the Natural Science Research Project of Higher Education Institutions of Jiangsu Province under Grant 20KJA470003; in part by the China Postdoctoral Science Foundation under Grant 2021M701647; and in part by the Priority Academic Program Development of Jiangsu Higher Education Institutions.

ABSTRACT In this article, a position sensorless control strategy for the five-phase interior permanent magnet synchronous motor (IPMSM) by injecting pseudo-random signal into the third harmonic space is proposed. The conventional sensorless control of five-phase IPMSM based on third harmonic space extracts rotor position signal by injecting high-frequency square voltage signals into the third harmonic space. However, high-frequency square-wave voltage injection (HFSVI) produces a loud audible noise. Different from the conventional HFSVI strategy, the proposed strategy injects simplified pseudo-random fixed-frequency phase-switching (SPRFFPS) signal into the third harmonic space of the five-phase IPMSM to reduce high-frequency audible noise. To verify the effectiveness of the proposed strategy, the power spectral density (PSD) of phase current is analyzed. Also, since high-frequency signal is not injected into the fundamental space, the digital filter in the fundamental space current loop will no longer be needed, which avoids time delay and degradation of control performance. Finally, the correctness of the proposed strategy is verified by experiments.

INDEX TERMS Five-phase interior permanent magnet synchronous motor, sensorless control, third harmonic space, pseudo-random signal injection.

I. INTRODUCTION

The interior permanent magnet synchronous motors (IPMSM) have the advantages of high efficiency, high torque density, high power density, etc [1], [2]. So it has been widely used in household appliances, electric vehicles, rail transportation, and other fields. With the improvement of power electronics, materials technology, and motor design [3], [4], multiphase motor control systems have made great development in recent years. Compared with conventional three-phase IPMSMs, five-phase motors have a variety of advantages: reducing the stator current without increasing the voltage per phase, increasing the torque per ampere for the same volume machine, improving the power density, reliability, and fault-tolerance [3], [5], [6], [7], [8]. In contrast to conventional three-phase motors, five-phase motors have the property of multiple harmonic spaces. Among these multiple harmonic spaces, the third harmonic space is more often used for fault tolerant control, sensorless control, etc [9], [10], [11], [12].

The accuracy of motor control systems depends on the rotor position signal which is usually extracted by a high-precision resolver or encoder. However, sensors cause a lot of impact on motor control systems. The presence of

The associate editor coordinating the review of this manuscript and approving it for publication was Zhuang Xu.

sensors not only increases the size of the control device and system cost but also reduces the reliability of the system [13]. For the above reasons, sensorless control technology has attracted the research interest of many scholars. Sensorless control is divided into two categories: First, methods based on a mathematical model of the motor which are applied in high speed range. Second, methods based on machine saliency which are used in low speed range [14]. In general, the position signal signal-to-noise ratio (SNR) of the model-based sensorless methods is dependent on the motor speed, and it is difficult to extract the motor position signals in low speed range. Therefore, model-based methods are only applicable to medium and high speeds [15].

Saliency-based sensorless control methods obtain the rotor position by tracking the rotor saliency. After injecting a high-frequency (HF) signal, the induced currents contain rotor position information on account of the saliency of the magnetic path [16], [17]. Depending on the form of injection signal, HF signal injection methods can be divided into two categories: rotating signal injection and pulsating signal injection, respectively. Among them, rotating signal injection requires the machine saliency of the motor and is mostly used in IPMSM. Pulsating signal injection can be used in both surface-mounted permanent magnet synchronous motors (SPMSM) and IPMSM because of its ability to excite the saturation saliency of the motor. According to the different types of injection signal, pulsating signal injection can be divided into pulsating sinusoidal injection method [16], [18], [19], [20], [21], and pulse square wave injection method, respectively [22].

Although the high-frequency injection method has good performance in low speed range, the audible noise cannot be ignored [23]. One of the most significant factors limiting the application of sensorless algorithms based on high-frequency signal injection is audible noise. To solve this problem, methods based on varying the amplitude and frequency of the injected signal have been proposed Low amplitude high-frequency signals can reduce noise, but the reduction in signal amplitude makes the SNR of the motor position signals escalate and thus affects the operating status of the motor [24], [25]. Another way to reduce audible noise is to bring the frequency of the injected signal into the inaudible range [15], [26], [27]. However, this method increases switching loss.

Following the idea of power conversion, the introduction of pseudo-random signal injection to reduce the audible noise method has received attention from scholars in recent years. There are two main types of pseudo-random signal injection: phase-switching and frequency-switching. Phase-switching pseudo-random signal injection reduces audible noise by randomly injecting HF signal with four different phases [28]. Different from phase-switching pseudo-random signal injection, two different frequencies HF signals are injected into motor randomly in frequency-switching pseudo-random signal injection. In [29] and [30], a pseudo-random frequency-switching high-frequency square-wave voltage injection method is proposed. Similarly, the random sinusoidal injection method with two different frequencies was proposed in [31]. Usually, analysis of the current power spectral density (PSD) for pseudo-random signal injection methods has been made. Audible noise is reduced by injecting random signals which can expand the current spectrum.

For five-phase IPMSM, there are some studies about the combination of the third harmonic space and sensorless control. However, few existing studies take audible noise into account [10], [32]. In this paper, a pseudo-random signal injection sensorless control strategy based on the third harmonic space is proposed. A simplified pseudo-random fixed-frequency phase-switching signal is injected into the third harmonic space of five-phase IPMSM to eliminate DC bias and reduce the audible noise of the motor. The rotor position is obtained by normalizing the current of the stationary $\alpha_3\beta_3$ reference frame in third harmonic space, which overcomes the inadequacy of the traditional sign function to mediate the rotor position information. The current spectrum and position estimation results are analyzed in the experimental results.

II. DECOUPLED MATHEMATICAL MODEL OF FIVE-PHASE IPMSM

To reduce the complexity of the control system and improve control efficiency, the space of the five-phase motor is decoupled into two mutually orthogonal and decoupled subspaces: the fundamental space and the third harmonic space. The two-axis systems are shown in Fig. 1, where $\alpha_1\beta_1$ axis and $\alpha_3\beta_3$ axis are the stationary reference frame in the fundamental space and third harmonic space, respectively. Obviously, the angular frequency of the rotating d_3q_3 reference frame in the third harmonic space is three times the angular frequency of the rotating d_1q_1 reference frame in the fundamental space.

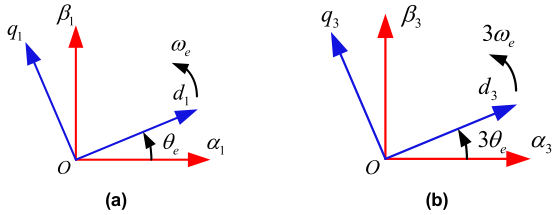

FIGURE 1. Positional relationship between two decoupled subspaces in five-phase IPMSM (a) fundamental space (b) third harmonic space [10].

According to the principle of constant amplitude before and after the transformation, the Clarke transformation matrix and the Park transformation matrix are written as:

$$T_{Clarke} = \begin{bmatrix} 1 & \cos\delta & \cos\delta & \cos\delta & \cos\delta \\ 0 & \sin\delta & \sin\delta & \sin\delta & \sin\delta \\ 1 & \cos 3\delta & \cos 3\delta & \cos 3\delta & \cos 3\delta \\ 0 & \sin 3\delta & \sin 3\delta & \sin 3\delta & \sin 3\delta \\ \frac{1}{\sqrt{2}} & \frac{1}{\sqrt{2}} & \frac{1}{\sqrt{2}} & \frac{1}{\sqrt{2}} & \frac{1}{\sqrt{2}} \end{bmatrix} \quad (1)$$

$$T_{\text{Park}} = \begin{bmatrix} \cos\theta_e & \sin\theta_e & 0 & 0 & 0 \\ -\sin\theta_e & \cos\theta_e & 0 & 0 & 0 \\ 0 & 0 & \cos 3\theta_e & \sin 3\theta_e & 0 \\ 0 & 0 & -\sin 3\theta_e & \cos 3\theta_e & 0 \\ 0 & 0 & 0 & 0 & 1 \end{bmatrix} \quad (2)$$

where θ_e is the electrical angle and δ is the spatial shifting angle between adjacent phases, being δ=$2\pi/5$. In (2), Two submatrices of the fifth-order Park transformation matrix are Park transformation matrices of fundamental space and third harmonic space, respectively. These two submatrices are located on the diagonal of the fifth-order Park transformation matrix.

The voltage equation of five-phase PMSM with third harmonic magnetic under d_1q_1 frame and d_3q_3 frame can be written as:

$$\begin{aligned} \begin{bmatrix} u_{d1} \\ u_{q1} \\ u_{d3} \\ u_{q3} \end{bmatrix} &= R \begin{bmatrix} i_{d1} \\ i_{q1} \\ i_{d3} \\ i_{q3} \end{bmatrix} + \begin{bmatrix} L_{d1} & 0 & 0 & 0 \\ 0 & L_{q1} & 0 & 0 \\ 0 & 0 & L_{d3} & 0 \\ 0 & 0 & 0 & L_{q3} \end{bmatrix} p \begin{bmatrix} i_{d1} \\ i_{q1} \\ i_{d3} \\ i_{q3} \end{bmatrix} \\ &+ \omega_e \begin{bmatrix} 0 & -L_{q1} & 0 & 0 \\ L_{d1} & 0 & 0 & 0 \\ 0 & 0 & 0 & -3L_{q3} \\ 0 & 0 & 3L_{d3} & 0 \end{bmatrix} \begin{bmatrix} i_{d1} \\ i_{q1} \\ i_{d3} \\ i_{q3} \end{bmatrix} \\ &+ \omega_e \begin{bmatrix} 0 \\ \psi_{m1} \\ 0 \\ 3\psi_{m3} \end{bmatrix} \end{aligned} \quad (3)$$

where u_{d1}, u_{q1}, i_{d1}, i_{q1}, L_{d1}, L_{q1}, ψ_{m1} are the voltage, current, inductance, and flux linkage in the fundamental space, respectively; u_{d3}, u_{q3}, i_{d3}, i_{q3}, L_{d3}, L_{q3}, ψ_{m3} are the voltage, current, inductance and the flux linkage in the third harmonic space; ω_e, R, p are the electrical angular velocity, stator resistance and the differential operator.

The fundamental space electromagnetic torque T_{e1} and the third harmonic space electromagnetic torque T_{e3} can be expressed as:

$$\begin{aligned} T_{e1} &= \frac{5}{2} P_n [\psi_{m1} i_{q1} + (L_{d1} - L_{q1}) i_{d1} i_{q1}] \\ T_{e3} &= \frac{5}{2} P_n [3\psi_{m3} i_{q3} + 3(L_{d3} - L_{q3}) i_{d3} i_{q3}] \\ T_e &= T_{e1} + T_{e3} \end{aligned} \quad (4)$$

where P_n is the number of pole pairs.

In five-phase IPMSMs, since the third harmonic permanent flux is not equal to zero, it is necessary to incorporate the third harmonic current into the double closed loop for control artificially. As shown in (4), the third harmonic torque pulsations can be eliminated by setting the third harmonic space current to zero, and the phase currents will not contain third harmonic components.

III. PROPOSED METHOD OF PSEUDO-RANDOM SIGNAL INJECTION SENSORLESS CONTROL BASED ON THIRD HARMONIC SPACE

A. PSEUDO-RANDOM SIGNAL INJECTION FOR POSITION SENSORLESS CONTROL OF FIVE-PHASE IPMSM BASED ON THIRD HARMONIC SPACE

The positional relationship between the estimated rotating reference frame and actual rotating reference frame in fundamental space and third harmonic space are shown in Fig. 2.

In Fig 2, the superscript "~" represents the difference between the estimated value and the actual value, and the superscript "^" represents the estimated value, respectively. $\hat{d}_1\hat{q}_1$ and $\hat{d}_3\hat{q}_3$ are the estimated rotating reference frame in the fundamental space and third harmonic space, respectively. $\tilde{\theta}_e = \hat{\theta}_e - \theta_e$ and $3\tilde{\theta}_e = 3\hat{\theta}_e - 3\theta_e$ are the angular estimation error in the fundamental space and third harmonic space, respectively.

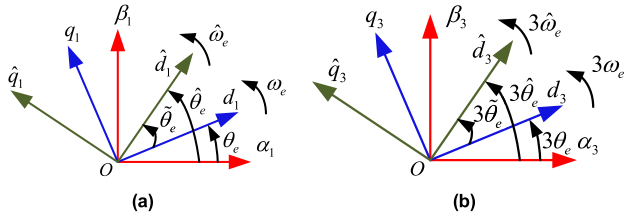

FIGURE 2. Positional relationship between estimated rotating reference frame and actual rotating reference frame in two decoupled subspaces (a) fundamental space (b) third harmonic space.

Since the frequency of the injection signal is much higher than the fundamental frequency of the motor, ignoring the stator resistance voltage and electromotive force, the HF voltage model of the five-phase IPMSM in the third harmonic space can be described as:

$$\begin{bmatrix} u_{d3h} \\ u_{q3h} \end{bmatrix} = \begin{bmatrix} L_{d3h} & 0 \\ 0 & L_{q3h} \end{bmatrix} p \begin{bmatrix} i_{d3h} \\ i_{q3h} \end{bmatrix} \quad (5)$$

where u_{d3h}, u_{q3h}, i_{d3h}, and i_{q3h} are the HF voltage and current in the third harmonic space, respectively; L_{d3h} and L_{q3h} are the HF inductance, and $p$is the differential operator.

The HF signal is injected into the estimated d_3 axis:

$$\begin{bmatrix} u_{\hat{d}3h} \\ u_{\hat{q}3h} \end{bmatrix} = \begin{bmatrix} u_{inj}(t) \\ 0 \end{bmatrix} \quad (6)$$

where $u_{\hat{d}3h}$, $u_{\hat{q}3h}$ are the HF voltage in the estimated d_3q_3 rotating frame, and $u_{inj}(t)$ is the HF injection signal. Substituting (6) into (5), the relationship between the estimated HF voltage and current in the estimated d_3q_3 rotating frame can be expressed as:

$$\begin{aligned} \begin{bmatrix} u_{\hat{d}3h} \\ u_{\hat{q}3h} \end{bmatrix} &= \begin{bmatrix} u_{inj}(t) \\ 0 \end{bmatrix} \\ &= R(3\tilde{\theta}_e) \begin{bmatrix} L_{d3h} & 0 \\ 0 & L_{q3h} \end{bmatrix} R^{-1}(3\tilde{\theta}_e) p \begin{bmatrix} i_{\hat{d}3h} \\ i_{\hat{q}3h} \end{bmatrix} \end{aligned} \quad (7)$$

where $i_{\hat{d}3h}$ and $i_{\hat{q}3h}$, are the HF current in the estimated d_3q_3 rotating frame, $R(\cdot)$ is the transformation matrix.

The estimated position can be obtained by separating HF current component in the estimated q_3 axis and controlling it to zero.

The block diagram of the proposed method is shown in Fig. 3. The control strategy consists of two main parts: the injection of pseudo-random signals and the extraction of position signals. The pseudo-random signal is injected into the estimated d_3 axis of the third harmonic space. Since the third harmonic space and fundamental space are mathematically orthogonal to each other, the injection operation in the third harmonic space can reduce the impact of the injected signal on fundamental frequency space, theoretically, which will help to improve the stability of the operation of the five-phase IPMSM. In addition, low-pass filters (LPFs) used to separate the HF currents in the fundamental space current control loop are no longer needed because the signal is not injected in the fundamental space. Also, the benefits of injecting HF signal into third harmonic space for the positional signal processing process are not to be ignored. As mentioned before, the third harmonic current is generally controlled to zero to reduce the third torque pulsation, which means that the fundamental frequency value of the third harmonic current is negligible, and the band-pass filters (BPFs) used to separate HF signal in position signal processing will no longer be needed.

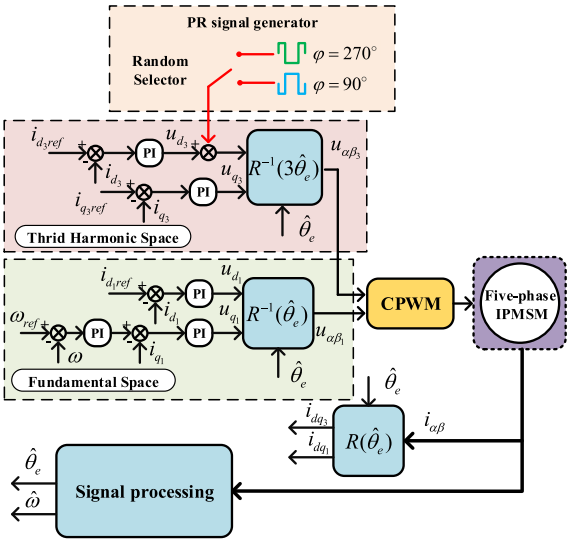

FIGURE 3. Control block diagram of the proposed pseudo-random signal injection for position sensorless control of five-phase IPMSM based on third harmonic space.

B. SIMPLIFIED PSEUDO-RANDOM FIXED-FREQUENCY PHASE-SWITCHING SIGNAL INJECTION SENSORLESS ALGORITHM

From (7), due to the existence of differential operators, the HF current response is related to the time integral value of the injection voltage. Suppose the time integral of the HF voltage is not zero for several consecutive cycles. In that case, it will produce DC bias in the estimated d_3 axis and lead to a discrepancy between the actual current value and the given value current in the estimated rotating reference frame current loop, which will have a negative effect on the operating

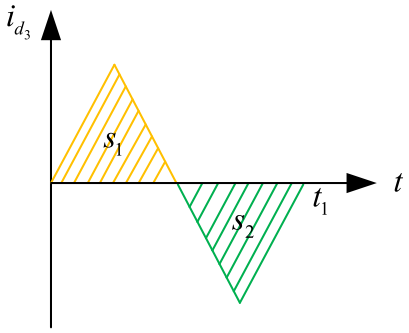

FIGURE 4. The HF current response of the injection voltage.

status of the motor. As shown in Fig. 4, s_1 represents the positive component of the current response and s_2 represents the negative component of the current response. s_1 must be equal to s_2 in a single injection cycle.

The conventional pseudo-random fixed-frequency phase-switching (PRFFPS) signal injection law is shown in (8):

$$PR(t, T_{inj}, \varphi) = \Re\{PR(t, T_{inj}, 0^\circ), PR(t, T_{inj}, 90^\circ), PR(t, T_{inj}, 180^\circ), PR(t, T_{inj}, 270^\circ)\} \quad (8)$$

where $\Re\{\}$, φ and T_{inj} are the random selection at every injection period, the phase of injection signal and the injection period, respectively. The variants of PRFFPS signal function are injection signal frequency, phase, and stochastic operator.

$$PR(t, T_{inj}, 0^\circ) = \begin{cases} V_{inj}, 0 \le t \le \dfrac{T_{inj}}{2} \\ -V_{inj}, \dfrac{T_{inj}}{2} < t \le T_{inj} \end{cases}$$

$$PR(t, T_{inj}, 90^\circ) = \begin{cases} 2V_{inj}, \dfrac{T_{inj}}{4} \le t \le \dfrac{3T_{inj}}{4} \\ -2V_{inj}, 0 \le t < \dfrac{T_{inj}}{4}, \dfrac{3T_{inj}}{4} < t \le T_{inj} \end{cases}$$

$$PR(t, T_{inj}, 180^\circ) = -PR(t, T_{inj}, 0^\circ)$$
$$PR(t, T_{inj}, 270^\circ) = -PR(t, T_{inj}, 90^\circ) \quad (9)$$

where V_{inj} is the amplitude of injection voltage.

In Fig. 5, the random signal function in (9) and its HF current response are displayed. It can be observed that the sum of the current response of the signals with 0° and 180° phase is not zero in a single injection cycle. As mentioned in Fig. 4, it leads to DC bias in the estimated rotating frame. There are two solutions to this problem. The first method is setting the probability of being selected of the 0° and 180° phase signals to be equal. Although it can theoretically make the total current response zero for several consecutive cycles, this method is unstable since it randomly adjusts the injection signal. In other words, there is no guarantee that the opposite phase signal will be injected after the 0° and 180° phase signals injection. The 0° phase and 180° phase signals are combined into one injection signal in the second method. However, this injection method reduces the frequency of the injection.

Thus, to satisfy the injection frequency requirement and effectively avoid the DC bias problem, simplified

pseudo-random fixed-frequency phase-switching signal (SPRFFPS) injection is proposed. The SPRFFPS signal can be written as:

$$PR_{SPRFFPS}(t, T_{inj}, \varphi) = \Re\{PR(t, T_{inj}, 90^\circ), PR(t, T_{inj}, 270^\circ)\} \tag{10}$$

The HF current response of the SPRFFPS signal i_{dh} can be expressed as:

$$i_{dh} = \sum_{k=1}^{\infty} [iPR_{SPRFFPS}(t - kT_{inj}, T_{inj}, \varphi)] \tag{11}$$

$$iPR_{SPRFFPS}(t, T_{inj}, \varphi) = \Re\{iPR(t, T_{inj}, 90^\circ), iPR(t, T_{inj}, 270^\circ)\} \tag{12}$$

where $iPR_{SPRFFPS}(t, T_{inj}, \varphi)$ is equivalent current response.

SPRFFPS injection scheme and corresponding current response in (10) and (11) are shown in Fig. 6.

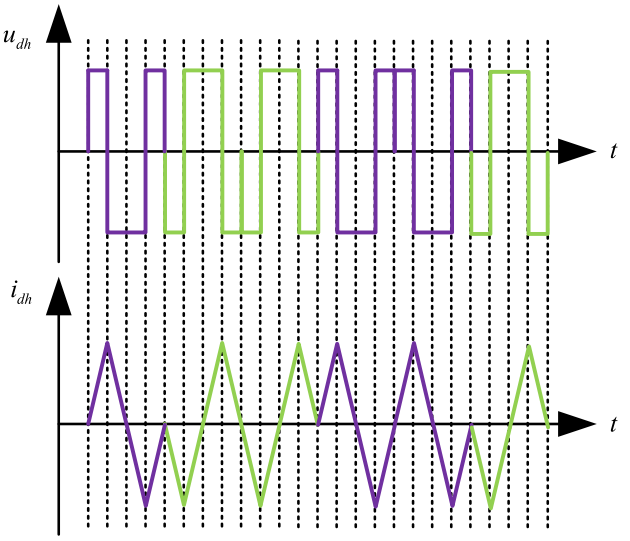

FIGURE 6. SPRFFPS injection scheme and corresponding current response.

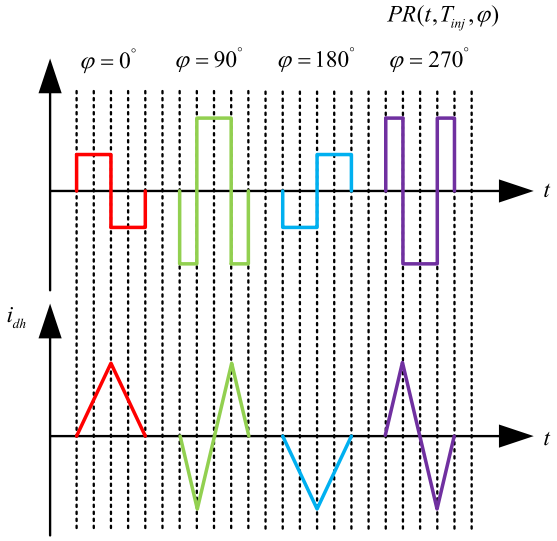

FIGURE 5. PRFFPS injection scheme and corresponding current response.

C. POSITION DEMODULATION ALGORITHM IN THIRD HARMONIC SPACE

The injection signal in the third harmonic space can be expressed as:

$$\begin{bmatrix} u_{\hat{d}3h} \\ u_{\hat{q}3h} \end{bmatrix} = \begin{bmatrix} u_{inj}(t) \\ 0 \end{bmatrix} = \begin{bmatrix} PR_{SPRFFPS}(t, T_{inj}, \varphi) \\ 0 \end{bmatrix} \tag{13}$$

Based on (7) and (13), the HF current response in the stationary $\alpha_3\beta_3$ reference frame can be expressed as:

$$\begin{bmatrix} i_{\alpha 3h} \\ i_{\beta 3h} \end{bmatrix} = \frac{\int PR_{SPRFFPS}(t, T_{inj}, \varphi)dt}{L^2 - \Delta L^2} \cdot \begin{bmatrix} L_{q3h}\cos 3\theta_e \cos 3\tilde{\theta}_e + L_{d3h}\sin 3\theta_e \sin 3\tilde{\theta}_e \\ L_{q3h}\sin 3\theta_e \cos 3\tilde{\theta}_e - L_{d3h}\cos 3\theta_e \sin 3\tilde{\theta}_e \end{bmatrix} \tag{14}$$

where $\int PR_{SPRFFPS}(t, T_{inj}, \varphi)dt$ is the time integral of the SPRFFPS signal which can be considered as a constant, $L = (L_{\mathrm{d3h}} + L_{\mathrm{q3h}})/2$ and $\Delta L = (L_{\mathrm{d3h}}\text{-}L_{\mathrm{q3h}})/2$. The HF current response in the estimated d_3q_3 rotating reference frame can be written as:

$$\begin{bmatrix} i_{\hat{d}3h} \\ i_{\hat{q}3h} \end{bmatrix} = R^{-1}(3\hat{\theta}_e) \begin{bmatrix} i_{\alpha 3h} \\ i_{\beta 3h} \end{bmatrix} = \frac{\int PR_{SPRFFPS}(t, T_{inj}, \varphi)dt}{L^2 - \Delta L^2} \cdot \begin{bmatrix} L_{q3h}\cos^2 3\tilde{\theta}_e + L_{d3h}\sin^2 3\tilde{\theta}_e + \Delta L \sin 6\tilde{\theta}_e \\ L_{q3h}\cos^2 3\tilde{\theta}_e + L_{d3h}\sin^2 3\tilde{\theta}_e - \Delta L \sin 6\tilde{\theta}_e \end{bmatrix} \tag{15}$$

When $\tilde{\theta}_e$ is small enough, (15) can be simplified as:

$$\begin{bmatrix} i_{\hat{d}3h} \\ i_{\hat{q}3h} \end{bmatrix} = \frac{\int PR_{SPRFFPS}(t, T_{inj}, \varphi)dt}{L^2 - \Delta L^2} \begin{bmatrix} L_{q3h} + \Delta L \sin 6\tilde{\theta}_e \\ L_{q3h} - \Delta L \sin 6\tilde{\theta}_e \end{bmatrix} \tag{16}$$

Due to the presence of negative values in the amplitude of the injected signal, to accurately obtain the rotor angular information, the absolute value of (16) can be written as:

$$\begin{bmatrix} \left|i_{\hat{d}3h}\right| \\ \left|i_{\hat{q}3h}\right| \end{bmatrix} = \frac{\left|\int PR_{SPRFFPS}(t, T_{inj}, \varphi)dt\right|}{L^2 - \Delta L^2} \begin{bmatrix} \left|L_{q3h} + \Delta L \sin 6\tilde{\theta}_e\right| \\ \left|L_{q3h} - \Delta L \sin 6\tilde{\theta}_e\right| \end{bmatrix} \tag{17}$$

where $L_{q3h} > \Delta L$, and $6\tilde{\theta}_e \approx 0$, (17) can be written as:

$$\begin{bmatrix} \left|i_{\hat{d}3h}\right| \\ \left|i_{\hat{q}3h}\right| \end{bmatrix} = \frac{\left|\int PR_{SPRFFPS}(t, T_{inj}, \varphi)dt\right|}{L^2 - \Delta L^2} \begin{bmatrix} L_{q3h} + \Delta L \sin 6\tilde{\theta}_e \\ L_{q3h} - \Delta L \sin 6\tilde{\theta}_e \end{bmatrix} \tag{18}$$

The current of stationary reference frame in third harmonic space after demodulation can be expressed as:

$$\begin{bmatrix} i_{\alpha 3hl} \\ i_{\beta 3hl} \end{bmatrix} = R(3\hat{\theta}_e) \begin{bmatrix} \left|i_{\hat{d}3h}\right| \\ i_{\hat{q}3h} \end{bmatrix} = \frac{\left|\int PR_{SPRFFPS}(t, T_{inj}, \varphi)dt\right|}{L^2 - \Delta L^2} \cdot \begin{bmatrix} L_{q3h} \cos 3\theta_e \cos 3\tilde{\theta}_e + L_{d3h} \sin 3\theta_e \sin 3\tilde{\theta}_e \\ L_{q3h} \sin 3\theta_e \cos 3\tilde{\theta}_e - L_{d3h} \cos 3\theta_e \sin 3\tilde{\theta}_e \end{bmatrix} \quad (19)$$

when $\tilde{\theta}_e \approx 0$, (19) can be simplified as:

$$\begin{bmatrix} i_{\alpha 3hl} \\ i_{\beta 3hl} \end{bmatrix} = \frac{\left|\int PR_{SPRFFPS}(t, T_{inj}, \varphi)dt\right|}{L^2 - \Delta L^2} \begin{bmatrix} L_{q3h} \cos 3\theta_e \\ L_{q3h} \sin 3\theta_e \end{bmatrix} = \frac{\left|\int PR_{SPRFFPS}(t, T_{inj}, \varphi)dt\right|}{L_{d3h}} \begin{bmatrix} \cos 3\theta_e \\ \sin 3\theta_e \end{bmatrix} \quad (20)$$

However, the HF injection voltage in an injection period is not constant during motor operation. The HF voltage will be distorted due to the hysteresis of the control system, the nonlinearity of the inverter, etc. Thus, the current signal needs to be normalized.

The normalized HF current response is given in (21).

$$\begin{bmatrix} i_{\alpha 3h\_n} \\ i_{\beta 3h\_n} \end{bmatrix} = \frac{1}{\sqrt{(i_{\alpha 3hl})^2 + (i_{\beta 3hl})^2}} \begin{bmatrix} i_{\alpha 3hl} \\ i_{\beta 3hl} \end{bmatrix} = \begin{bmatrix} \cos 3\theta_e \\ \sin 3\theta_e \end{bmatrix} \quad (21)$$

The position error ε can be calculated as:

$$\varepsilon = i_{\beta 3h\_n} \cos 3\hat{\theta}_e - i_{\alpha 3h\_n} \sin 3\hat{\theta}_e = \sin 3\tilde{\theta}_e \quad (22)$$

If the position error is small enough, (22) can be rewritten as:

$$\varepsilon = \sin 3\tilde{\theta}_e \approx 3\tilde{\theta}_e \quad (23)$$

Position signal can be obtained by controlling the error ε to zero through the phase phase-locked loop (PLL). Because this position demodulation algorithm is based on the third harmonic space, the estimated rotor angular velocity and position values are both three times fundamental space values. The control block diagram of the position demodulation algorithm in the third harmonic space is shown in Fig. 7.

D. CURRENT PSD ANALYSIS OF SPRFFPS SCHEME

Power Spectral Density (PSD) is a signal analysis method that can be used to convert a time domain signal to the frequency domain when analyzing a time series to visualize the variation/variance (energy) as a function of frequency.

The PSD shows at which frequencies the data variation is large, which is useful to further analyze the current frequency energy distribution. In the field of motor control, PSD is an effective tool for analyzing the phase current spectrum [28]. The current PSD spectrum can be written as:

$$S(f) = f_i \left\{ E_\varphi \left[|I(f)|^2 \right] - \left| E_\varphi [I(f)] \right|^2 + f_i \left| E_\varphi [I(f)] \right|^2 \sum_{k=-\infty}^{\infty} \delta(f - kf_i) \right\} \quad (24)$$

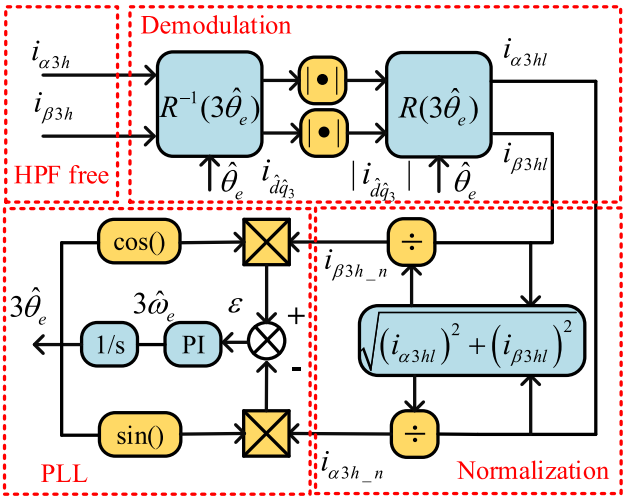

FIGURE 7. Control block diagram of position demodulation algorithms in third harmonic space.

where the operator $E[]$ denotes the mathematical expectation operation, $I(f)$ represents the Fourier expansion of HF currents, f_i is the injected signal frequency and $\delta(f)$ is the unit impulse function.

Assuming that the induced current consists of currents with different frequencies at phase 90° and 270°, the Fourier transform of the HF current can be written as:

$$I_{90^\circ}(f) = -\frac{2 - 2\cos(f\pi T_{RES}) - f\pi T_{RES} \sin(f\pi T_{RES})}{f^2\pi^2 T_{RES}} e^{-j\pi f T_{RES}} \quad (25)$$

$$I_{270^\circ}(f) = \frac{2 - 2\cos(f\pi T_{RES}) - f\pi T_{RES} \sin(f\pi T_{RES})}{f^2\pi^2 T_{RES}} e^{-j\pi f T_{RES}} \quad (26)$$

Since the frequencies of the individual harmonics in the Fourier analysis are multiples of the fundamental frequency, bringing $f = nf_{RES}$ into (25) and (26):

$$I_{T_{RES}}(f) = \begin{cases} 0 & when\ n\ is\ even \\ \dfrac{-4}{\pi^2 n^2 f_{RES}} & when\ n\ is\ odd \end{cases} \quad (27)$$

From (27), although there is a discrete component in the current response of the SPRFFPS, it can be canceled out by the phase difference of the signal. Since the two phase signals have the same probability of injection, the total mathematical expectation of the current is zero, and the discrete part of the (24) can be written as:

$$E_\varphi [I(f)] = \sum_{k=1}^{+\infty} P(k) I_k(f) = 0 \quad (28)$$

Bringing (28) into (24), it can be concluded that the current PSD under SPRFFPS signal injection does not contain discrete components, which are the source of the audible noise.

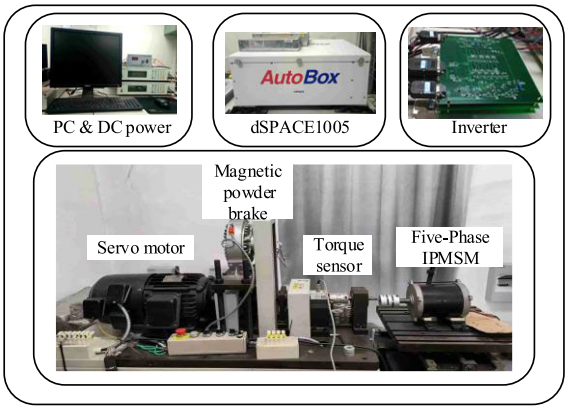

FIGURE 8. Experimental platform of Five-Phase IPMSM drive.

IV. EXPERIMENTAL RESULTS VERIFICATION

To verify the suitability of the proposed five-phase IPMSM method, a test platform has been set up as shown in Fig. 8. The experiment set is composed of a five-phase permanent magnet machine, a five-phase half-bridge inverter, and a servo motor as the load. The dSPACE1005 controller is utilized for the implementation of the overall control algorithm. The parameters of the machine are presented in Table 1. The machine torque is measured by a high-precision torque ransducer (HBM T20WN/20NM). The frequency of PWM is fixed at 10 kHz, and the DC-link voltage is 50 V. The injection frequency is set to 1250 Hz and the magnitude of the injected HF voltages is 20 V for 90° and 270° phase injection signals.

TABLE 1. Practical parameter of five-phase IPMSM.

Pole-pairs	4
Fundamental permanent magnet flux linkage	0.111 Wb
Third harmonic permanent magnet flux linkage	1.3×10^{-3} Wb
Stator phase resistance	0.8 Ω
Fundamental d-axis inductance	5.3 mH
Fundamental q-axis inductance	17 mH
Third harmonic d-axis inductance	1.91 mH
Third harmonic q-axis inductance	1.97 mH
Rated speed	1500 r/min

TABLE 2. Comparison of current psd with different injection strategies.

injection strategies	Spectral peaks (dB)				
	1.25kHz	3.75kHz	6.25kHz	8.75kHz	10kHz
1250Hz fixed frequency	-12	-31.2	-41.6	-49.5	-32.2
1250Hz SPRFFPS	-26.5	-50.5	-54.5	-58	-32.2

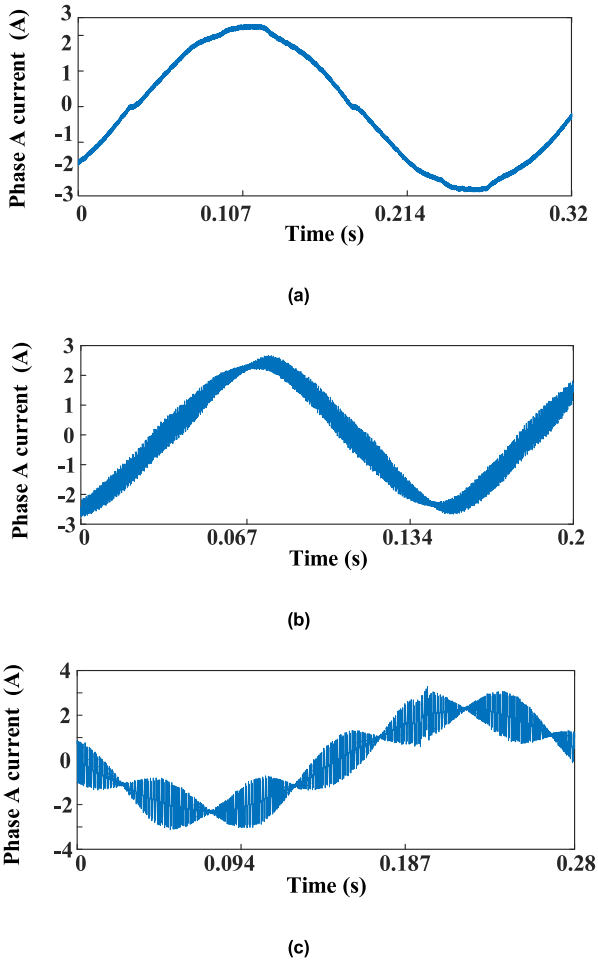

FIGURE 9. Experimental results of phase A current under different injection signals (a) no signal injection (b) SPRFFPS signal injection into fundamental space (c) SPRFFPS signal injection into third harmonic space.

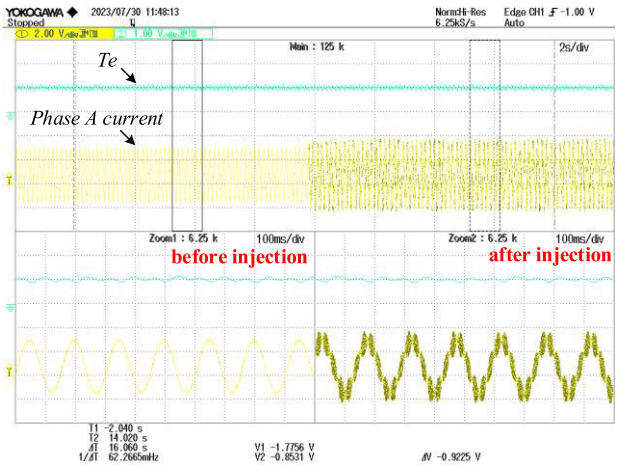

FIGURE 10. Comparison of phase A currents before and after SPRFFPS signal injection in the third harmonic space; *Te* is scaled to 2.5 Nm/div, phase A current is scaled to 2 A/div.

Firstly, in order to verify the correctness of signal injection, SPRFFPS signal is injected into the fundamental space as well as third harmonic space to compare the waveforms of the phase currents. Phase A current with no injection, with the SPRFFPS injection in fundamental space, and with the SPRFFPS injection in third harmonic space are shown in

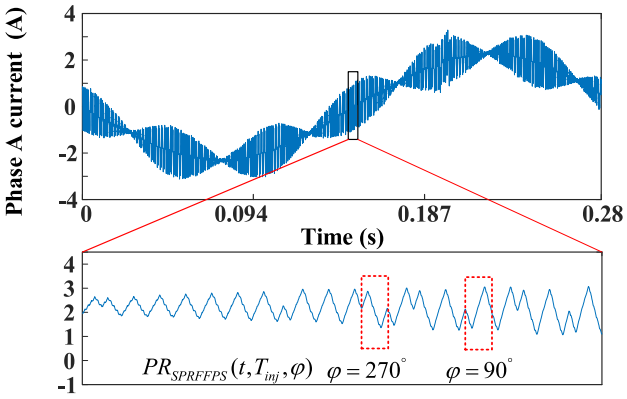

FIGURE 11. Experimental results of position demodulation algorithms in the third harmonic space.

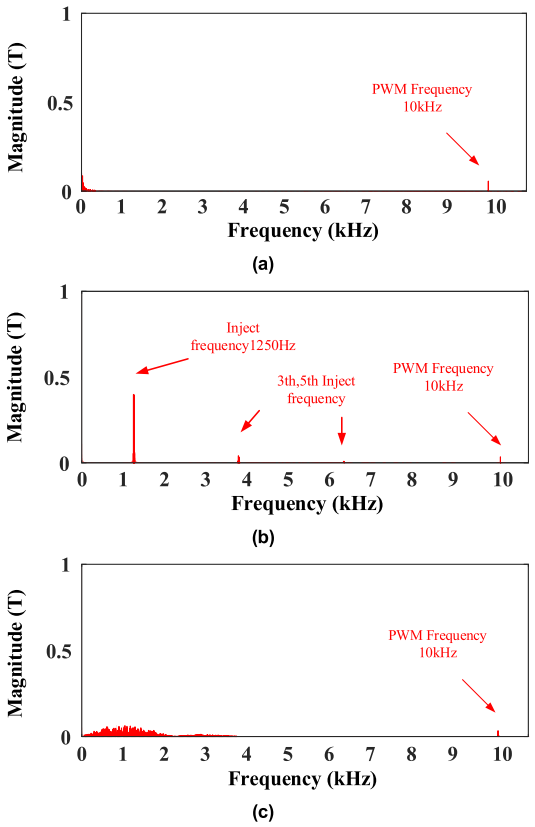

FIGURE 12. Phase current FFT analysis (a) no signal injection (b) fixed-frequency signal injection into third harmonic space (c) SPRFFPS signal injection into third harmonic space.

Fig. 9 (a), (b), (c), respectively. The focus is on comparing A phase current response after the SPRFFPS signal injection into fundamental space and third harmonic space. As shown in Fig. 9 (b), response current of injection signal fluctuates once during one-half of the electrical cycle of phase A current (crest to adjacent trough of current waveforms). However, in Fig. 9 (c), fluctuation of the response current of injection signal during one-half of the electrical cycle of phase A current are three times. Fig. 10 results phase A current before and

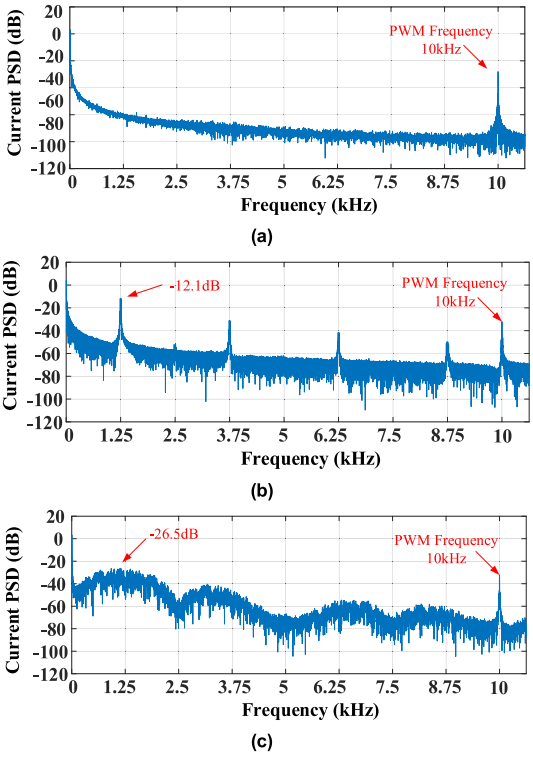

FIGURE 13. Phase current PSD analysis (a) no signal injection (b) fixed-frequency signal injection into third harmonic space (c) SPRFFPS signal injection into third harmonic space.

after SPRFFPS signal injection into third harmonic space at speed of 50 rpm and load torque of 2.5 Nm. The difference in the amplitude of A phase current before and after the injection is due to the superposition of the response current of injection signal on the phase current. Compared with no injection, the A phase current after the SPRFFPS signal injection obviously contains harmonic currents with three fundamental frequency fluctuations. Thus, this is in accordance with the description of triple frequency relationship between fundamental space and third harmonic space in part A of section II. It can be determined that HF voltages are indeed injected into third harmonic space of the motor. In addition, there is no significant change in the torque waveform before and after the injection, which can verify that the injection signal in third harmonic space has less effect on the torque. The waveforms of the motor phase currents after the injection of the SPRFFPS signal also need to be verified, as shown in Fig. 11. The response current of 90° phase and 270° phase signals appear randomly in A phase currents, and have the same form as analysed in Fig. 6. Therefore, the SPRFFPS signal is correctly injected into third harmonic space of the motor.

Fig. 12 and Fig. 13 show experimental phase current FFT analysis with the PSD in different injection modes (no signal injection, fixed-frequency signal injection into third harmonic space and the SPRFFPS signal injection into third harmonic space). In Fig. 12 (b), The spectral peaks are mainly concentrated at odd multiples of the injected signal frequency and decrease with increasing frequency.

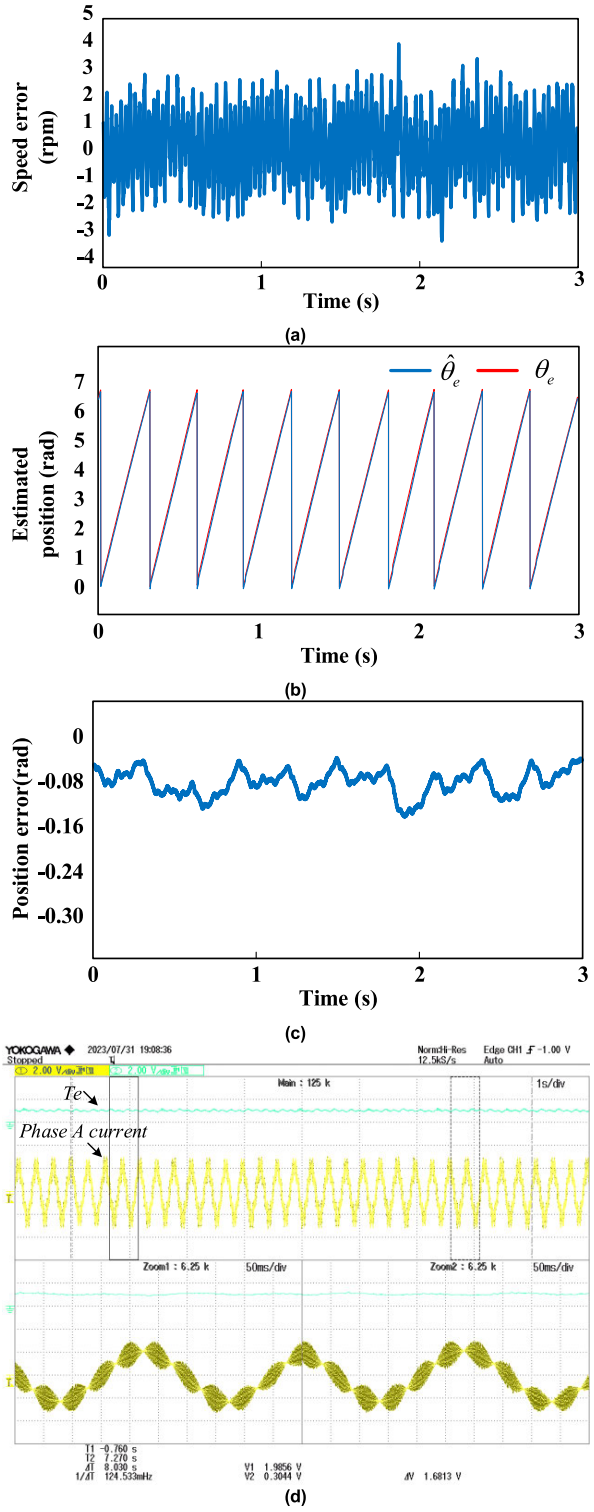

FIGURE 14. Sensorless performance experiment results at 50 rpm with 2.5 Nm load (a) speed error (b) estimated and real position (c) position error (d) phase A current and torque; *Te* is scaled to 5 Nm/div, phase A current is scaled to 2 A/div.

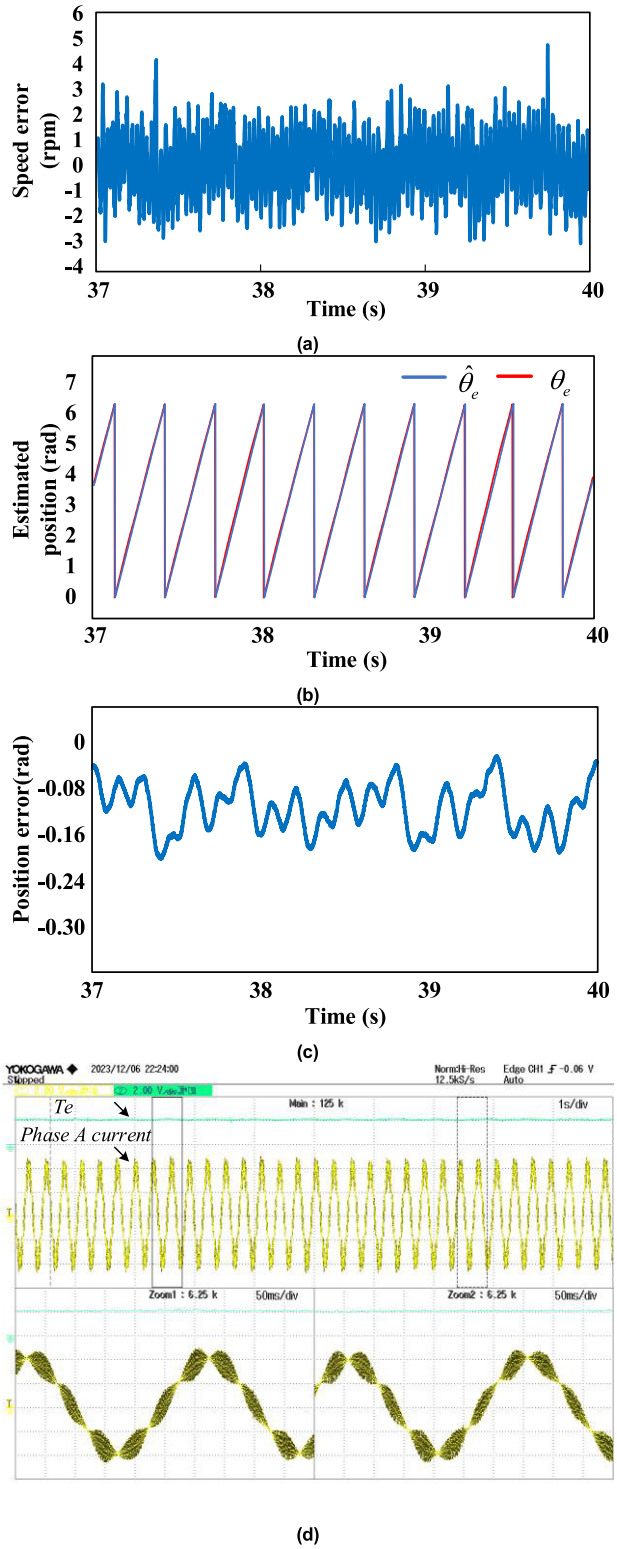

FIGURE 15. Sensorless performance experiment results at 50 rpm with 5 Nm load (a) speed error (b) estimated and real position (c) position error (d) phase A current and torque; *Te* is scaled to 5 Nm/div, phase A current is scaled to 2 A/div.

In Fig. 12 (c), The spectral peaks at odd multiples of the injected signal frequency are largely spread over neighboring frequencies, which directly contributes to the dispersion of the signal energy.

In Fig. 13 (a), since no injection signal, the PSD of the motor phase currents has a large amplitude only at the PWM frequency. However, In Fig. 13 (b), with the injection of

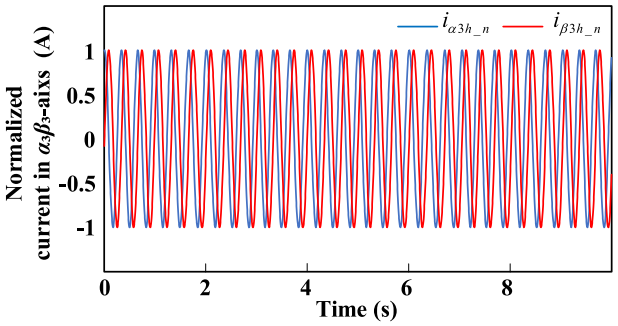

FIGURE 16. Experiment result of the normalized $\alpha_3\beta_3$-axis current.

fixed-frequency signals, discrete spectra appear in the phase current PSD, and these harmonic discrete spectra are the main source of audible noise. In addition, the PSD continuous spectrum amplitude of Fig. 13 (b) is higher than the PSD continuous spectrum amplitude of Fig. 13 (a) due to the extra energy brought by the signal injection. In Fig. 13 (c), compared with fixed-frequency injection, the SPRFFPS signal have a broad continuous spectrum and lower audible noise. That is, the energy of the discrete harmonic spectrum is dispersed in the adjacent continuous harmonic spectrum. This demonstrates the effectiveness of the SPRFFPS injection strategy in reducing current audible noise.

Table 2 compares the noise of the two injection methods at specific current frequencies. Compared with fixed-frequency injection, the discrete spectrum of SPRFFPS injection decreases by approximately 14.5 dB for 1.25 kHz and 19.3 dB for 3.75 kHz injection.

Fig. 14 shows sensorless performance experiment results at 50 rpm with 2.5 Nm load. The floating value of the speed estimation error is around 6 rpm and maximum value of the position estimation error is around 0.16 rad, and the mean value of the error product remains around 0.1 rad. Fig. 15 shows sensorless performance experiment results at 50 rpm with 5 Nm load. The speed error fluctuates around 6 rpm, while the maximum and average position errors are around 0.24 rad and 0.15 rad. The experiment result of the demodulated normalized $\alpha_3\beta_3$-axis current is shown in Fig. 16.

V. CONCLUSION

In this paper, SPRFFPS signal injection for position sensorless control of five-phase IPMSM based on third harmonic space is proposed. The proposed method reduces audible noise by broadening the current spectrum and also removes filters from the fundamental space current loop and third harmonic space loop, which reduces the delay of the control system. Compared to fixed-frequency signal injection, the SPRFFPS signal injection causes a less discrete spectrum of phase current PSD. Also, the SPRFFPS signal injection method avoids DC bias by selecting the 90° and 270° phase voltage signals randomly. With the proposed position demodulation algorithm, the rotor position can be extracted from the third harmonic space. Current PSD and sensorless position estimation performance are demonstrated on a 2kw five-phase IPMSM platform.

REFERENCES

[1] G. Zhang, G. Wang, D. Xu, R. Ni, and C. Jia, "Multiple-AVF cross-feedback-network-based position error harmonic fluctuation elimination for sensorless IPMSM drives," *IEEE Trans. Ind. Electron.*, vol. 63, no. 2, pp. 821–831, Feb. 2016.
[2] R. Antonello, L. Ortombina, F. Tinazzi, and M. Zigliotto, "Enhanced low-speed operations for sensorless anisotropic PM synchronous motor drives by a modified back-EMF observer," *IEEE Trans. Ind. Electron.*, vol. 65, no. 4, pp. 3069–3076, Apr. 2018.
[3] Q. Chen, W. Zhao, G. Liu, and Z. Lin, "Extension of virtual-signal-injection-based MTPA control for five-phase IPMSM into fault-tolerant operation," *IEEE Trans. Ind. Electron.*, vol. 66, no. 2, pp. 944–955, Feb. 2019.
[4] Q. Chen, G. Xu, G. Liu, W. Zhao, L. Liu, and Z. Lin, "Torque ripple reduction in five-phase IPM motors by lowering interactional MMF," *IEEE Trans. Ind. Electron.*, vol. 65, no. 11, pp. 8520–8531, Nov. 2018.
[5] X. Sun, K. Diao, G. Lei, Y. Guo, and J. Zhu, "Study on segmented-rotor switched reluctance motors with different rotor pole numbers for BSG system of hybrid electric vehicles," *IEEE Trans. Veh. Technol.*, vol. 68, no. 6, pp. 5537–5547, Jun. 2019.
[6] X. Sun, Z. Shi, G. Lei, Y. Guo, and J. Zhu, "Analysis and design optimization of a permanent magnet synchronous motor for a campus patrol electric vehicle," *IEEE Trans. Veh. Technol.*, vol. 68, no. 11, pp. 10535–10544, Nov. 2019.
[7] M. J. Duran and F. Barrero, "Recent advances in the design, modeling, and control of multiphase machines—Part II," *IEEE Trans. Ind. Electron.*, vol. 63, no. 1, pp. 459–468, Jan. 2016.
[8] F. Barrero and M. J. Duran, "Recent advances in the design, modeling, and control of multiphase machines—Part I," *IEEE Trans. Ind. Electron.*, vol. 63, no. 1, pp. 449–458, Jan. 2016.
[9] J. Li, B. Du, T. Zhao, S. Wu, and S. Cui, "Current sensor fault-tolerant control for five-phase PMSM drives based on third-harmonic space," *IEEE Trans. Ind. Electron.*, vol. 69, no. 10, pp. 9827–9837, Oct. 2022.
[10] G. Liu, C. Geng, and Q. Chen, "Sensorless control for five-phase IPMSM drives by injecting HF square-wave voltage signal into third harmonic space," *IEEE Access*, vol. 8, pp. 69712–69721, 2020.
[11] G. Liu, Z. Lin, W. Zhao, Q. Chen, and G. Xu, "Third harmonic current injection in fault-tolerant five-phase permanent-magnet motor drive," *IEEE Trans. Power Electron.*, vol. 33, no. 8, pp. 6970–6979, Aug. 2018.
[12] S. Dwari and L. Parsa, "Fault-tolerant control of five-phase permanent-magnet motors with trapezoidal back EMF," *IEEE Trans. Ind. Electron.*, vol. 58, no. 2, pp. 476–485, Feb. 2011.
[13] D. Liang, J. Li, R. Qu, and W. Kong, "Adaptive second-order sliding-mode observer for PMSM sensorless control considering VSI nonlinearity," *IEEE Trans. Power Electron.*, vol. 33, no. 10, pp. 8994–9004, Oct. 2018.
[14] G. Wang, M. Valla, and J. Solsona, "Position sensorless permanent magnet synchronous machine drives—A review," *IEEE Trans. Ind. Electron.*, vol. 67, no. 7, pp. 5830–5842, Jul. 2020.
[15] S. Kim, J.-I. Ha, and S.-K. Sul, "PWM switching frequency signal injection sensorless method in IPMSM," *IEEE Trans. Ind. Appl.*, vol. 48, no. 5, pp. 1576–1587, Sep./Oct. 2012.
[16] S.-I. Kim, J.-H. Im, E.-Y. Song, and R.-Y. Kim, "A new rotor position estimation method of IPMSM using all-pass filter on high-frequency rotating voltage signal injection," *IEEE Trans. Ind. Electron.*, vol. 63, no. 10, pp. 6499–6509, Oct. 2016.
[17] L. Chen, G. Götting, S. Dietrich, and I. Hahn, "Self-sensing control of permanent-magnet synchronous machines with multiple saliencies using pulse-voltage-injection," *IEEE Trans. Ind. Appl.*, vol. 52, no. 4, pp. 3480–3491, Jul. 2016.
[18] M. J. Corley and R. D. Lorenz, "Rotor position and velocity estimation for a salient-pole permanent magnet synchronous machine at standstill and high speeds," *IEEE Trans. Ind. Appl.*, vol. 34, no. 4, pp. 784–789, Jul. 1998.
[19] X. Zhang, H. Li, S. Yang, and M. Ma, "Improved initial rotor position estimation for PMSM drives based on HF pulsating voltage signal injection," *IEEE Trans. Ind. Electron.*, vol. 65, no. 6, pp. 4702–4713, Jun. 2018.
[20] Q. Tang, A. Shen, X. Luo, and J. Xu, "PMSM sensorless control by injecting HF pulsating carrier signal into ABC frame," *IEEE Trans. Power Electron.*, vol. 32, no. 5, pp. 3767–3776, May 2017.
[21] X. Luo, Q. Tang, A. Shen, and Q. Zhang, "PMSM sensorless control by injecting HF pulsating carrier signal into estimated fixed-frequency rotating reference frame," *IEEE Trans. Ind. Electron.*, vol. 63, no. 4, pp. 2294–2303, Apr. 2016.

[22] Y.-D. Yoon, S.-K. Sul, S. Morimoto, and K. Ide, "High-bandwidth sensorless algorithm for AC machines based on square-wave-type voltage injection," *IEEE Trans. Ind. Appl.*, vol. 47, no. 3, pp. 1361–1370, May 2011.
[23] B. Du, T. Zhao, S. Han, L. Song, and S. Cui, "Sensorless control strategy for IPMSM to reduce audible noise by variable frequency current injection," *IEEE Trans. Ind. Electron.*, vol. 67, no. 2, pp. 1149–1159, Feb. 2020.
[24] A. A. Khan and O. Mohammed, "Neural network based modeling of audible noise for high frequency injection based position estimation for PM synchronous motors at low and zero speed," in *Proc. IEEE Electric Ship Technol. Symp.*, Apr. 2009, pp. 119–122.
[25] Y. Tauchi and H. Kubota, "Audible noise reduction method in IPMSM position sensorless control based on high-frequency current injection," in *Proc. Int. Power Electron. Conf. (IPEC-Hiroshima-ECCE ASIA)*, May 2014, pp. 3119–3123.
[26] Z. Ma, J. Gao, and R. Kennel, "FPGA implementation of a hybrid sensorless control of SMPMSM in the whole speed range," *IEEE Trans. Ind. Informat.*, vol. 9, no. 3, pp. 1253–1261, Aug. 2013.
[27] W. Qian, X. Zhang, F. Jin, H. Bai, D. Lu, and B. Cheng, "Using high-control-bandwidth FPGA and SiC inverters to enhance high-frequency injection sensorless control in interior permanent magnet synchronous machine," *IEEE Access*, vol. 6, pp. 42454–42466, 2018.
[28] G. Wang, H. Zhou, N. Zhao, C. Li, and D. Xu, "Sensorless control of IPMSM drives using a pseudo-random phase-switching fixed-frequency signal injection scheme," *IEEE Trans. Ind. Electron.*, vol. 65, no. 10, pp. 7660–7671, Oct. 2018.
[29] G. Wang, L. Yang, B. Yuan, B. Wang, G. Zhang, and D. Xu, "Pseudo-random high-frequency square-wave voltage injection based sensorless control of IPMSM drives for audible noise reduction," *IEEE Trans. Ind. Electron.*, vol. 63, no. 12, pp. 7423–7433, Dec. 2016.
[30] G. Wang, L. Yang, G. Zhang, X. Zhang, and D. Xu, "Comparative investigation of pseudorandom high-frequency signal injection schemes for sensorless IPMSM drives," *IEEE Trans. Power Electron.*, vol. 32, no. 3, pp. 2123–2132, Mar. 2017.
[31] G. Zhang, G. Wang, H. Wang, D. Xiao, L. Li, and D. Xu, "Pseudorandom-frequency sinusoidal injection based sensorless IPMSM drives with tolerance for system delays," *IEEE Trans. Power Electron.*, vol. 34, no. 4, pp. 3623–3632, Apr. 2019.
[32] J. Li, B. Du, T. Zhao, Y. Cheng, and S. Cui, "Sensorless control of five-phase permanent-magnet synchronous motor based on third-harmonic space," *IEEE Trans. Ind. Electron.*, vol. 69, no. 8, pp. 7685–7695, Aug. 2022.

YUHAO ZHANG received the B.Sc. degree in automation from the Anhui University of Technology, Ma'anshan, China, in 2017. He is currently pursuing the M.Sc. degree in control engineering with Jiangsu University, Zhenjiang, China.

His current research interests include electric machines, motor drives, and sensorless control.

CHEN CHEN received the B.Sc. and M.S. degrees in control science and engineering from North China Electric Power University, Baoding, China, in 2009 and 2012, respectively.

He is currently with the Electrical Design Institute, China Nuclear Power Engineering Company Ltd. (CNPE), engaged in electrical design and research of nuclear power plant electrical systems. His research interests include the application and research of variable frequency speed regulation technology in large circulate water pumps of nuclear power plants, and medium voltage multi-pole low-speed special motors in large circulate water pumps of nuclear power plants.

ZHENGMENG LIU (Member, IEEE) received the B.Sc. degree in electrical engineering from Chongqing University, Chongqing, China, in 2013, the M.S. degree in electrical engineering from Jiangsu University, Zhenjiang, China, in 2016, and the Ph.D. degree in electrical engineering from The University of Sheffield, Sheffield, U.K., in 2021.

Since 2021, he has been with Jiangsu University, where he is currently a Lecturer with the School of Electrical Information Engineering. His research interests include the design and analysis of permanent magnet electrical machines and linear actuators.

QIAN CHEN (Senior Member, IEEE) received the B.Sc. and Ph.D. degrees in electrical engineering and control engineering from Jiangsu University, Zhenjiang, China, in 2009 and 2015, respectively.

Since 2015, he has been with Jiangsu University, where he is currently a Professor with the School of Electrical Information Engineering. From 2020 to 2021, he was a Visiting Professor with the Department of Electronic and Electrical Engineering, The University of Sheffield, Sheffield, U.K. His current research interests include electric machine design, modeling, fault analysis, and intelligent control. He is a Full Member of Sigma Xi, The Scientific Research Honor Society.

JIAHAO ZHANG received the B.Sc. degree in electrical automation from the Yancheng Institute of Technology, Yancheng, China, in 2018, and the M.S. degree from Jiangsu University, Zhenjiang, China, in 2021, where he is currently pursuing the Ph.D. degree in control science and engineering.

His research interests include high-performance control of electric machines and position sensorless control.

GUOHAI LIU (Senior Member, IEEE) received the B.Sc. degree from Jiangsu University, Zhenjiang, China, in 1985, and the M.Sc. and Ph.D. degrees in electrical engineering and control engineering from Southeast University, Nanjing, China, in 1988 and 2002, respectively.

Since 1988, he has been with Jiangsu University, where since 2002, he has been a Professor with the School of Electrical Information Engineering. He is currently the Director of the Jiangsu Key Laboratory of Drive and Intelligent Control for Electric Vehicles. From 2003 to 2004, he was a Visiting Professor with the Department of Electronic and Electrical Engineering, The University of Sheffield, Sheffield, U.K. His teaching and research interests include electrical machines, motor drives for electric vehicles (EV), and intelligent control. He has authored or coauthored more than 300 technical articles and four textbooks and is the holder of 80 patents in these areas.

Prof. Liu is a fellow of the Institution of Engineering and Technology (IET), U.K.